Research Article Open Access

Shouyun Zhang* and Jinghong Ma*

Study on the unsaturated hydrogen bond behavior of bio-based polyamide 56

https://doi.org/10.1515/epoly-2019-0004
Received June 15, 2018; accepted October 23, 2018.

Abstract: In this paper, the unsaturated hydrogen bonds (H-bonds) of the bio-based polyamide 56 (PA56) with an odd-even unit structure were analyzed by infrared spectroscopy. It was proved that the bio-based PA56 had less saturated H-bonds, which became attenuated and blue-shifted at the temperature exceeding 260°C. Besides, as H-bond was decayed and broken, new unsaturated H-bonds readily formed. Moreover, the experimental results obtained strongly indicate that the unsaturated H-bonds of bio-based polyamide 56 could react with polar metal oxides. Besides, the intercalation of montmorillonite was found to have a significant influence on the hydrogen bond between polymer chains.

Keywords: bio-based polyamide 56; hydrogen bond; variable temperature infrared spectroscopy; two-dimensional infrared spectroscopy

1 Introduction

Polyamide is a polymer, which has been widely used in the production of plastics, fibers, and other materials. Due to the presence of amide groups in molecular chains of polyamide, its supramolecular structure and properties are strongly affected by intramolecular and intermolecular hydrogen bonds (H-bonds). The latter are bonds between electron-deficient hydrogen and a region of high electron density, which play a crucial role in determining the shapes, properties, and functions of biomolecules. Bio-based polyamide 56 (PA56) is synthesized by the polymerization process of glutamine and adipic acid. It has attracted considerable attention because of its environmental friendliness (1-3).

Molecular unit structures of PA56 (in contrast to those of PA6 and PA66 polyamides) exhibit an odd-even asymmetry pattern. Thus, the N-H and C=O polar groups in the macromolecule chain segment are in dislocation state, which will lead to the decrease of hydrogen bonding and the increase of unsaturated H-bonds. The structure of polyamide 56 endows its unique crystallization and thermodynamic properties.

Hao et al. (4) characterized the structure and thermal properties of PA56 utilizing differential scanning calorimetry (DSC) and X-ray diffraction (XRD). It was found that PA56 had lower glass transition temperature and a higher melting point, as compared to PA6 and PA66. Moreover, the uniformities of the distribution and agglomeration state of macromolecular segments were both weaker than those of polyamides with an even-even structure. Morales-Gámez et al. (5) studied the effect of H-bonds on the crystalline behavior of PA56 during the heating process and found that the conformation and cell size of PA56 were different from those of PA6 and PA66, and the crystalline morphology of PA56 was only slightly affected by the crystallization conditions. Kuo et al. (6) studied the change of H-bond strength by the differential scanning calorimetry (DSC) and infrared spectroscopy. It was concluded that the relative position and distance between polar groups forming H-bonds in polymers had the significant influence on the strength and stability of H-bonds. In general, shorter relative position distances and a smaller degree of dislocation tend to form H-bonds with higher strength and stability.

Variable temperature Fourier transform infrared (FTIR) spectroscopy and two-dimensional infrared correlation spectroscopy have been widely used in the study on the H-bonding and intermolecular interactions. Chu et al. (7) analyzed the effect of nano-$CaCO_3$ particles

*** Corresponding authors: Shouyun Zhang and Jinghong Ma,** State Key Laboratory for Modification of Chemical Fibers and Polymer Materials, College of Materials Science and Engineering, Donghua University, Shanghai, China, e-mail: Syzhang2008741208@163.com and mjh68@dhu.edu.cn.

on the solid-state transition and crystallization-related bands of PET in PET/$CaCO_3$ blends using variable temperature infrared spectroscopy. The results showed that the addition of nano-$CaCO_3$ particles significantly improved the crystallization and melting behavior of PET. Peng et al. (8) studied the variation order and relationship of different polar groups of PA6 during heating by the two-dimensional infrared correlation spectroscopy. It was found that the H-bond of PA6 exhibited an apparent bond dissociation and attenuation at higher temperatures. The number of H-bonds was first decreased, and then that of unsaturated groups was increased. At the same time, no new H-bonds were found. Montmorillonite (MMT) is mainly composed of particles with a negative polarity. Nano-sized zinc oxides also obtain a strongly manifested polarity via their surface processing. Thus, montmorillonite and zinc oxide nanopowders have good reactivities with high H-bonding of the polymer.

Meanwhile, intercalation formed by the montmorillonite have an essential effect on H-bonding strength and stability. Such additives play a significant role in polymer' s properties. For example, they can improve the strength, toughness, and ultraviolet radiation resistance of PA56 products. Chu et al. (7) investigated the interaction between H-bonding and the metal compounds or polarity ions. Wang (9) studied the effect of montmorillonite intercalation on the performance of PET polymer. The results showed that adding montmorillonite can abate the interaction between polymer molecules' group and reduce the topology structure of the macromolecular chain segment, which was beneficial for the macromolecular orientation degree and lower crystallinity, as well as improved the strength, elongation at break, and toughness of the product. However, there are only a few reports on the changes in H-bonds of PA56 during the heating process and the interaction between PA56 and metal oxides and montmorillonite based on the infrared spectroscopy, while such findings are significant for the application and modification of PA56.

In this paper, the change of H-bonding in polyamide 56 during the heating process was analyzed by the variable temperature infrared spectroscopy (FTIR) and two-dimensional infrared spectroscopy. The differences in the H-bond behavior in PA56 with an odd-even structure and PA6 or PA66 with even-even structure were examined. Besides, the effects of montmorillonite and zinc oxide on the H-bond interaction of bio-based polyamide 56 were also discussed.

2 Materials

Bio-based PA56 chips (fiber grade) with the number average molecular weight (i.e., total weight of the sample divided by the number of molecules in the sample) of about 2.29×10^5 were purchased from DuPont Co., Ltd. PA 6 chips (fiber grade) with number-average molecular weight about 2.31×10^5 were purchased from Li Peng Co., Ltd, Taiwan. PA66 chips (fiber grade) with the number average molecular weight of about 2.30×10^5 were purchased from Suzhou Nilit Co., Ltd. Formic acid (purity 99.2%) was obtained from Chongqing East Chemical Group Co., Ltd. Montmorillonite (MMT) masterbatch containing 30 wt% montmorillonite and 70 wt% PA56 was obtained from Zhejiang Fenghong New Material Co., Ltd. Zinc oxide (ZnO) masterbatch containing 25 wt% ZnO and 75 wt% PA56 was purchased from Jiangsu Kaihong New Material Technology Co., Ltd. The diameters of the zinc oxide nanopowders and montmorillonite were 20 nm and 25 μm, respectively. Their surfaces were negatively polarized.

3 Sample preparation and test procedures

3.1 The preparation of mixed samples

PA 56 chips were dried at 140°C for 10 h in the nitrogen atmosphere. The moisture content in the chips was about 430 ppm after drying. Montmorillonite and zinc oxide masterbatches were dried in vacuum drum at 120°C for 8 h and melt-blended with PA 56 chips by the double cone micromixer to prepare PA56/MMT blends and PA56/ZnO blends, respectively.

3.2 FTIR characterization

PA56, PA6, and PA66 were dissolved in formic acid, and the concentration of the solution was 5%, respectively. The solutions were heated to evaporate the solvent. Then the obtained solids were frozen for 1 h and ground to powders. The polyamide samples were analyzed by FTIR (Nicolet 6700, Thermo Fisher) in a KBr flake. The scanning range was 4000 to 400 cm^{-1}, the resolution was 1 cm^{-1}, and the scanning frequency was 45 times. Variable temperature - FTIR spectra were carried out at 16, 60, 120, 240, 260, and 280°C, respectively. 2D FTIR spectra were carried out at 20°C (16-290°C) by 2D IR Spectroscopy type (PhaseTech Spectroscopy Inc., US).

4 Results and discussion

4.1 Infrared analysis

FTIR spectra of polyamide samples tested at room temperature are depicted in Figure 1. The positions and corresponding groups of characteristic peaks in FTIR spectra are listed in Table 1. The absorption peaks at 1640 cm^{-1} and 1540 cm^{-1} are assigned to the stretching vibration peak of C=O (absorption peak of amide I) and the in-plane bending vibration peak of C=O (absorption peak of amide II) in the main chain of the polyamide, respectively. The absorption peaks at 3090 cm^{-1}, 3320 cm^{-1}, and 3450 cm^{-1} are assigned to H-bonded N-H groups in the crystalline part, H-bonded N-H group in the amorphous region, and free N-H group with no H-bond formation, respectively. As compared to PA6 and PA66, the absorption peak of PA56 at 3450 cm^{-1} is more obvious, indicating a higher amount of free N-H groups with no H-bond formation (10,11). Because of the unique odd-even structure of PA56, more N-H and C=O groups in the macromolecular chains are in the dislocation state, while the H-bonding is reduced. Therefore, the number of groups in the unsaturated H-bonding state without H-bonding is increased.

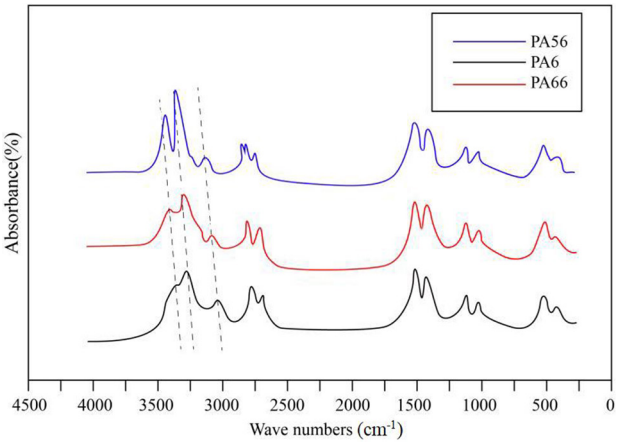

Figure 1: FTIR spectra of polyamides at room temperature.

Table 1: Positions and corresponding groups of characteristic peaks in FTIR spectra.

Groups	Corresponding wave number
The absorption peak of amide II	1540 cm^{-1}
The absorption peak of amide I	1640 cm^{-1}
Absorption peaks of $-CH_2-$ group in crystalline part	2860 cm^{-1}
The absorption peak of $-CH_2-$ group in the amorphous region	2930 cm^{-1}
The absorption peak of hydrogen-bonded N-H groups in crystalline part	3090 cm^{-1}
The absorption peak of hydrogen-bonded N-H group in the amorphous region	3320 cm^{-1}
Absorption peaks of free N-H group with no H-bond formation	3450 cm^{-1}

Figure 2 depicts the variable temperature FTIR spectra of polyamide samples at different temperatures (16, 60, 120, 240, 260, and 280°C). When the temperature increased from 16 to 240°C, no apparent changes in the wave number and intensity of the absorption peak at 3320 cm^{-1} corresponding to the H-bonded N-H group in the amorphous region could be found for the PA56 sample. The blue shift of this absorption peak occurred at 260°C. However, for PA6 and PA66 samples with even-even H-bonds, the absorption peak of the H-bond in the amorphous region exhibited a blue shift at 240°C. This implies that the odd-even H-bond in PA56 shows higher thermal stability at high temperature, while the dissociation of even-even H-bonds in PA6 and PA66 easily happens (12,13).

It can also be concluded from the analysis of Figure 2 that absorption peaks at 3450 cm^{-1} corresponding to the free N-H group without H-bond for PA6 and PA66 samples became more evident with the temperature increase. At lower temperatures, N-H groups in PA6 and PA66 usually formed H-bonds. Higher temperatures aggravated the dissociation of H-bonds, leading to a rise in the number of free N-H groups. In contrast, there was a slight change in the intensity of this absorption peak for a PA56 sample during the heating process. On the one hand, the number of H-bonds formed in PA 56 at lower temperatures was lower due to the asymmetry of the odd-even structure, making the absorption peaks at 3450 cm^{-1} more pronounced. On the other hand, during the H-bond decay process, the PA56 macromolecule can easily form a new H-bond with higher bond energy (10,11).

Two-dimensional infrared synchronous spectra of polyamide are shown in Figure 3. During the heating process of PA6 and PA66 samples, H-bond in H-bonded N-H group in the amorphous region at 3320 cm^{-1}) exhibited a weak negative correlation with unsaturated H-bond of free N-H group without no H-bond formation at 3450 cm^{-1}. Meanwhile, in the case of PA56, H-bond and unsaturated hydrogen manifested an apparent negative correlation. This can be attributed to the fact that the C=O and N-H groups are distributed regularly in the macromolecular chain because of the even-even structure of PA6 and PA66, resulting in the formation of H-bonds, instead of unsaturated ones. Meanwhile, the C=O and N-H groups of PA56 with odd-even structure are arranged in a dislocation mode in the macromolecule chain, which

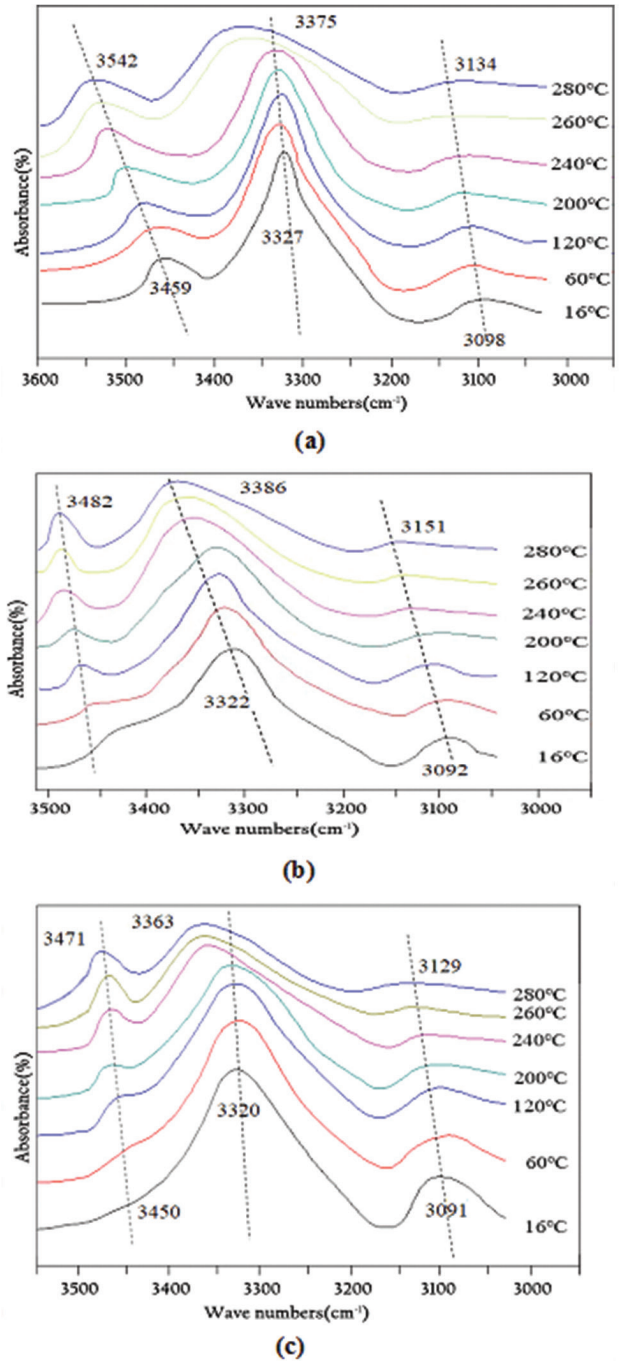

Figure 2: Variable temperature FTIR spectra of polyamide: (a) PA6; (b) PA66; (c) PA56.

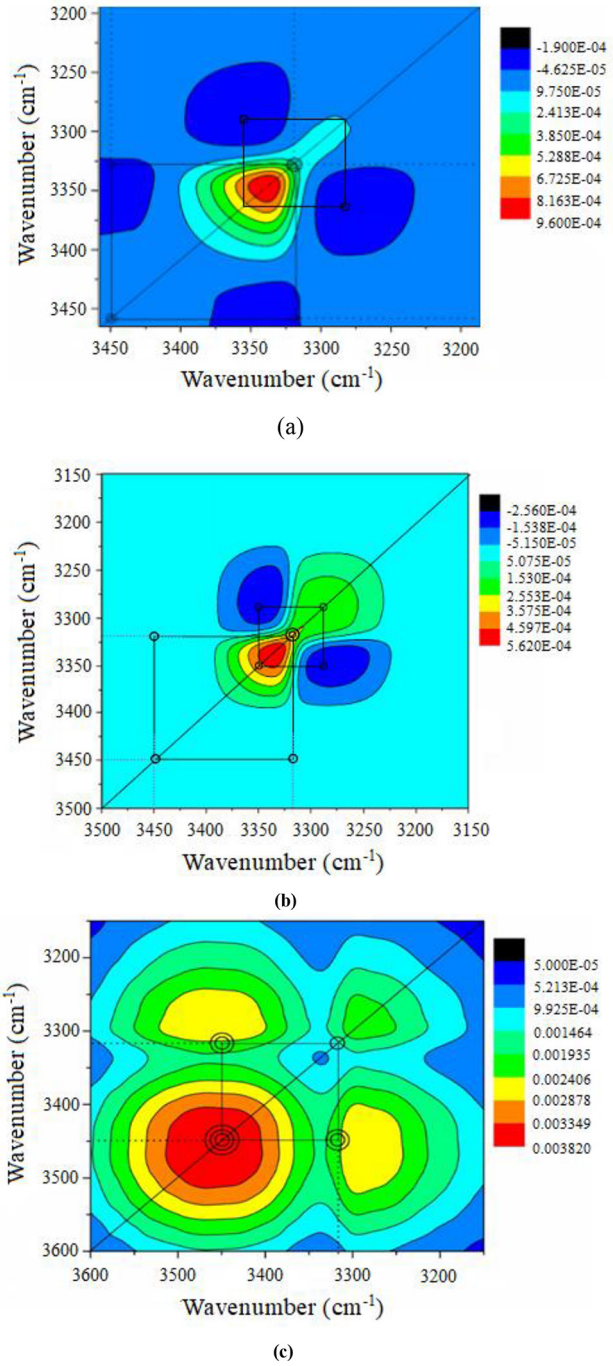

Figure 3: Two-dimensional infrared synchronous spectra of polyamide: (a) PA56; (b) PA6; (c) PA66.

led to the emergence of less saturated H-bonds (14,15). Because of the even-even structure of P polyamide polymer, H-bond strength is even, and when the H-bond is fractured, generally, new H-bonds are not formed. However, the H-bonds in odd-even structure polyamide polymer show a dislocation configuration, implying that their strength and stability are different. When the H-bonds are ruptured, those with higher strength are formed. Thus, two-dimensional infrared spectra of PA56 samples show no significant negative correlation. The H-bond groups in the even-even polyamide show better uniformity and stability since they are arranged regularly in the molecular chain. When the H-bond is disconnected, the unsaturated H-bond group is hard to form into new H-bond. So the H-bond and unsaturated H-bond show the apparent negative correlation. However, the polar groups

of an odd-even polymer are random, which implies that the molecular chains are prone to intertwine with each other. When the H-bonding is disconnected, the unsaturated H-bond can form a new high-strength H-bonding at the same time. So H-bond and unsaturated H-bond of PA56 samples show non-significant negative correlation (6,8).

Figure 4 shows two-dimensional infrared asynchronous spectra of polyamide samples. In PA6 and PA66, H-bonds were dissociated first during the heating process, and then the unsaturated H-bond was formed. In other words, the number of H-bonds was firstly reduced, and then the number of unsaturated H-bonds was increased. However, for PA56, the dissociation of H-bonds and the change of unsaturated H-bond number did not occur in an obvious order. When the even-even structures of PA6 and PA66 are subjected to high temperature, new H-bonds are rarely formed. In contrast, for PA56, because of the dissociation of H-bonds at high temperature, it is likely to slip for the macromolecular segment. Thus, the originally unsaturated H-bonds easily formed new H-bonds.

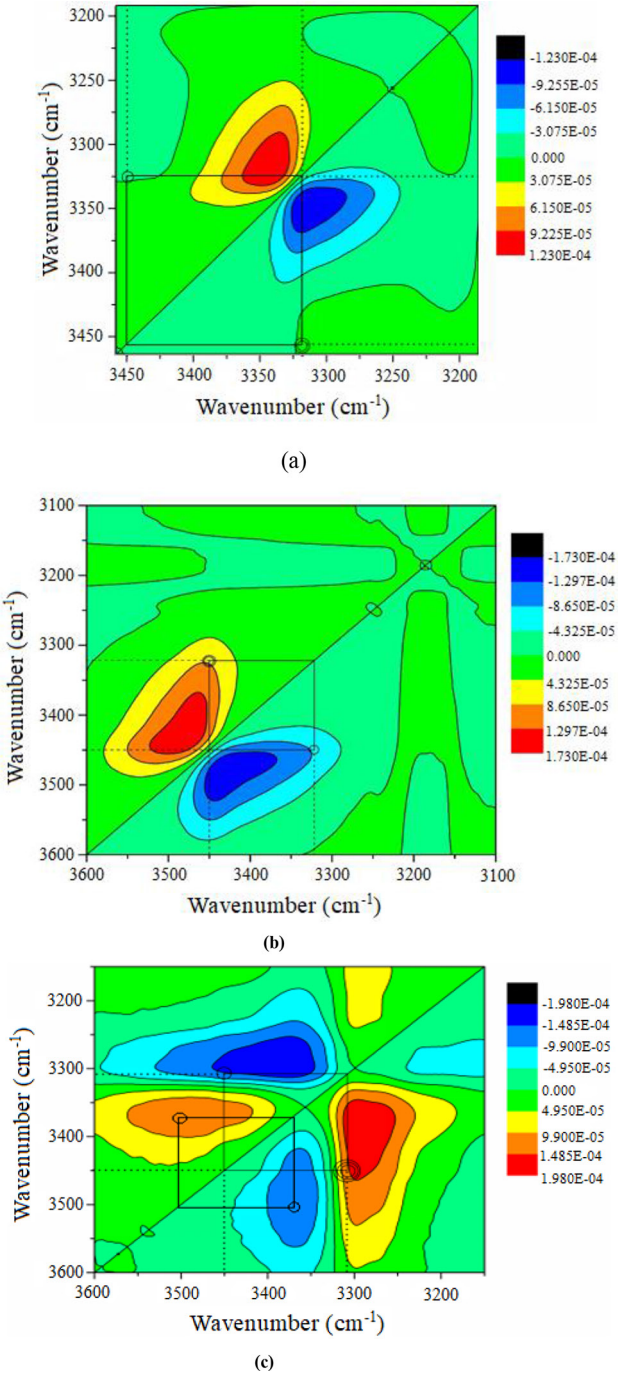

Figure 4: Two-dimensional infrared asynchronous spectra of polyamide polymers: (a) PA56; (b) PA6; (c) PA66.

4.2 The effect of montmorillonite on the H-bond interaction of bio-based polyamide 56

PA56/MMT blends were prepared by the melting mixing method. The effect of MMT on the H-bonding of PA 56 was studied by infrared spectroscopy. Figure 5 depicts FTIR spectra of PA56/MMT blends at room temperature. As the content of MMT of the blends increased, the absorption peak at 3320 cm^{-1} corresponding to the H-bonded N-H group in the amorphous region showed an apparent blue shift, while the absorption peaks at 3450 cm^{-1} corresponding to the free N-H group showed a blue shift. It is probably because the intercalation structure of MMT weakened the H-bond between PA56 groups and strengthened the free state of unsaturated H-bond (12,13). According to the reports on the montmorillonite-modified PA6 (12,16), the addition of MMT can form the intercalation structures in the polymer matrix and can weaken the interaction between the H-bond groups. At the same time, it can also

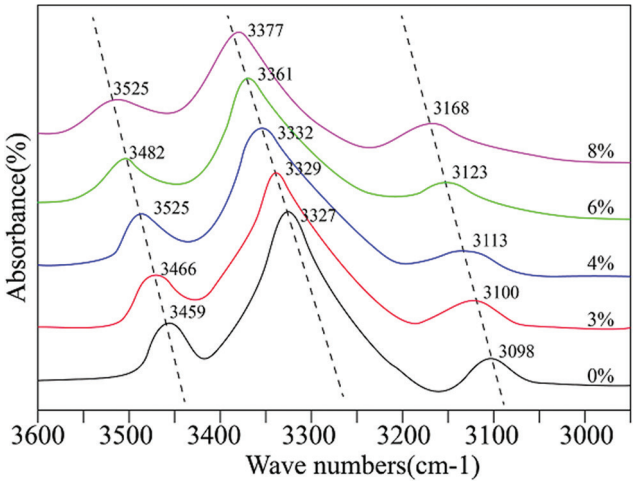

Figure 5: FTIR infrared spectra of PA56/MMT blends with different MMT contents at room temperature.

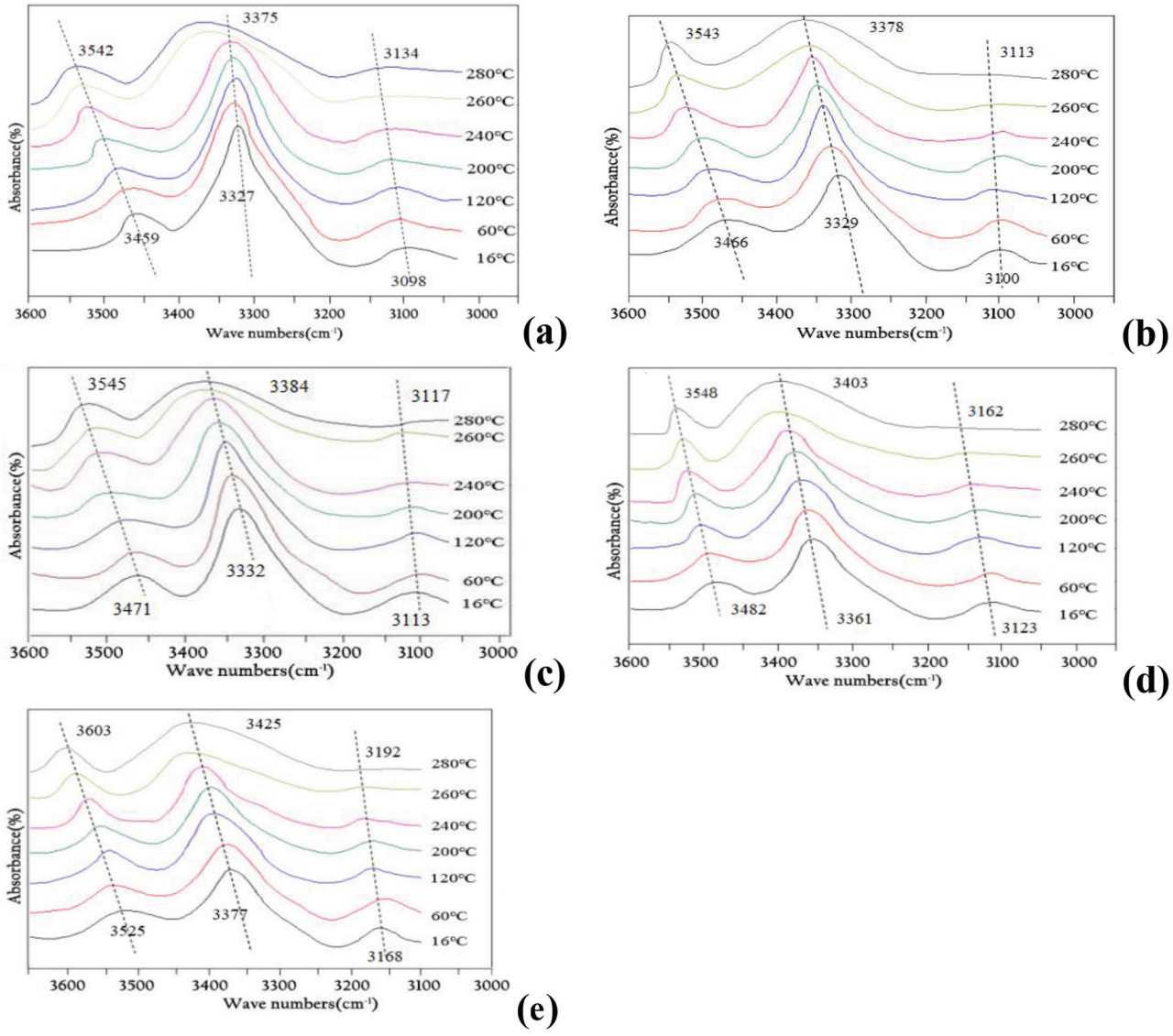

Figure 6: Variable temperature FTIR spectra of PA56/MMT blends with different MMT contents: (a) 0%; (b) 5%; (c) 8%; (d) 10%; (e) 12%.

strengthen the free state of unsaturated H-bond (12,13). This will be conducive to improve the toughness and orientation of high polymer (17,18).

Figure 6 depicts variable temperature FTIR spectra of PA56/MMT blends. For the blend with 5% MMT, the absorption peak of the H-bond at 3320 cm^{-1} does not exhibit an apparent blue shift below 240°C, which is similar to PA56. However, for the blends containing higher contents of MMT (8, 10, and 12%), the blue shift of the absorption peaks appears at low temperatures, and the wave number gradually increases during the heating process. This indicates that the intercalation of montmorillonite further weakens the interaction between polar groups and enhances their motion frequency (13,14). According to the literature, it will be helpful to improve toughness and orientation of fiber in the processing (19,20). With an increase in the montmorillonite content, the H-bond at 3320 cm^{-1} and the unsaturated H-bond at 3450 cm^{-1} exhibit an apparent blue shift at low temperatures. According to the results of Li et al. (16) and Cui et al. (17) on the effect of montmorillonite on the thermal infrared spectra of polymer, the intercalated montmorillonite weakens the force between H-bond groups and hinder the formation of a new H-bond.

4.3 The interaction between the polar nano-zinc oxide and bio-based PA56 unsaturated H-bonds

Figure 7 depicts the variable temperature FTIR spectra of PA56/ZnO blends. The absorption peak of the H-bond at 3320 cm^{-1} for the PA56/ZnO blends exhibited a shift at

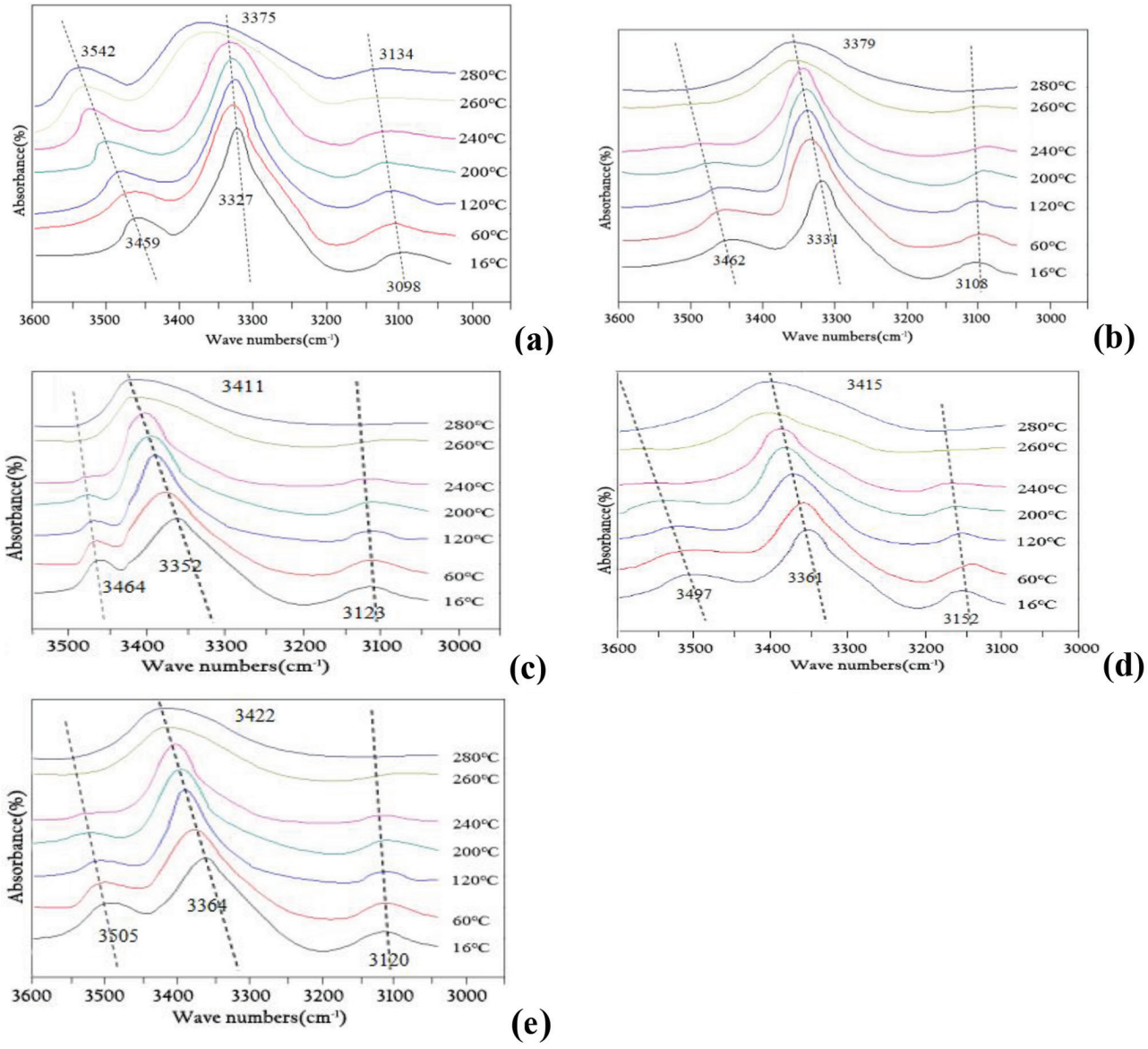

Figure 7: Variable temperature FTIR spectra of PA56/ZnO blends with different MMT contents: (a) 0%; (b) 1.0%; (c) 1.5%; (d) 2.0%; (e) 2.5%.

low temperature even for the minimal content of ZnO. The blue shift phenomenon became more pronounced with an increase in temperature, which indicated that nano-polar zinc oxide had a strong effect on PA56. Moreover, the intensity of absorption peak at 3450 cm^{-1} corresponding to the free N-H group decreased with the increase of temperature. Insofar as the interaction between the N-H polar group in PA56 macromolecule and the surface-negative nano-zinc oxide metal compound generated a certain coordination saturation effect between the polar groups of PA56 (18-20), the probability of H-bond formation was reduced, the decay of H-bond was accelerated, and the polarity of an unsaturated H-bond was neutralized. According to studies (21-23), the negative nano-zinc oxide could react with N-H polar groups, which reduced the H-bond strength and the degree of freedom of unsaturated H-bond. Therefore, the H-bond exhibited a strongly manifested blue shift at lower temperatures, while the characteristic peak of H-bond became less pronounced. With an increase in the amount of ZnO, this trend became more obvious. It is noteworthy that the characteristic peak almost did not change when the amount of ZnO reached 2.0%.

Figure 8 shows infrared spectra of polyamide 56 containing the appropriate proportion of polar nano-zinc oxide. Infrared analyses of the blend samples at different temperatures and infrared spectra at the same temperature (room temperature) were carried out. As seen in the

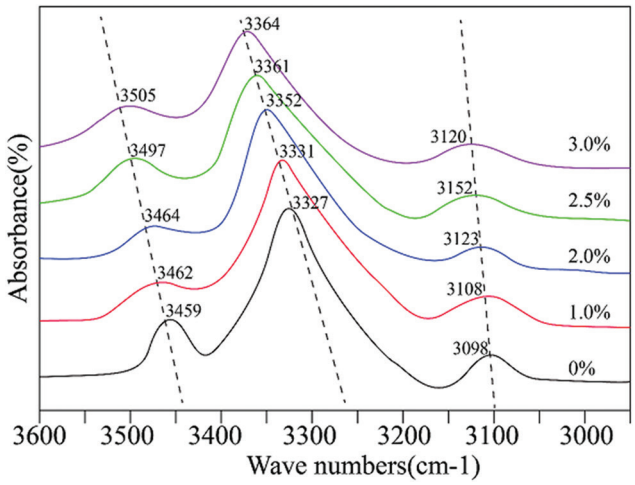

Figure 8: FTIR infrared spectra of PA56/ZnO blends with different ZnO contents at room temperature.

figures, the absorption peaks of the H-bond at 3320 cm^{-1} and unsaturated H-bonds at 3450 cm^{-1} exhibit a blue shift. In consideration of the better spinnability and the corresponding infrared test, the optimal ranges of the modified dosage of masterbatch and modifier are 8-10% and 2.0-2.5%, respectively. The infrared analysis revealed that blue shift became more pronounced at higher shares of polar nano-zinc oxide is higher, indicating that the modification is more effective (13,14). This is because zinc oxide displays a negative polarity by the surface modification, which reacts with C=O and N-H polar groups of bio-based polyamide 56 polymer molecules. As a result, the formation of H-bonds is reduced, and the polarity of unsaturated H-bonds is weakened, resulting in a particular coordination saturation effect between polar groups of bio-based polyamide 56 polymer macromolecules (21-23).

5 Conclusions

The bio-based PA56 has more unsaturated H-bonds, and the H-bonds are also unstable. When the H-bonds in the polymer were attenuated and cracked, new H-bonds were readily formed.

The unsaturated H-bond of the bio-based PA56 can interact with polar metal compounds. Besides, the montmorillonite has a strong influence on the H-bond strength. When montmorillonite was added to bio-based PA56 macromolecule polymer as a kind of polarized material, it could reduce the interaction strength of H-bonding between macromolecular chain segments and the unsaturated H-bonds. The montmorillonite intercalation reduced the interference of unsaturated H-bonds. Therefore, the stability of H-bonds was increased. It was found that the characteristic peak of H-bonds and the unsaturated H-bond exhibited a significant blue shift. The effect became more pronounced with an increase in the amount of montmorillonite up to 10%, after which saturation was observed.

Meanwhile, blue shifts were observed in the characteristic peaks of H-bond and unsaturated H-bonds when nano-zinc oxide was added to the samples. This trend was intensified until the amount of ZnO reached 2.0%. In samples with the addition of montmorillonite or nano-zinc oxide, H-bond exhibited a blue shift at lower temperatures during the heating process, implying that the thermal stability of the samples was deteriorated.

References

1. Wang Y., Kang H.L., Wang R., Liu R.G., Hao X.M., Crystallization of polyamide 56/polyamide 66 blends: Non-isothermal crystallization kinetics. J Appl Polymer Sci, 2018, 135(26), 46409.
2. Yan Y., Gooneie A. Ye H., Deng L., Qiu Z., Reifler F. A., et al., Morphology and crystallization of biobased polyamide 56 blended with polyethylene terephthalate. Macromol Mater Eng, 2018, 303(9), 36-42.
3. Zhang S., Ma J., Improvement of color value of bio-based polyamide 56 fibers. e-Polymers, 2018, 18(1), 91-95.
4. Hao X.M., Guo Y.F., Li Y.L., Yang Y., Shen Y., Hao X., et al., Study on the structure and properties of novel bio-based polyamide56 fiber compared with normal polyamide fibers. International Conference on Materials, Environmental and Biological Engineering, 2015.
5. Morales-Gámez L., Soto D., Franco L., Puiggalí J., Brill transition and melt crystallization of nylon 56: An odd-even polyamide with two hydrogen-bonding directions. Polymer, 2010, 51(24), 5788-5798.
6. Kuo S.W., Chan S.C., Chang F.C., Effect of H-bonding strength on the micro-structure and crystallization behavior of crystalline polymer blends. Macromolecules, 2003, 36(17), 6653-6661.
7. Chu Y.H., Wang J.W., Zhang B.G, Zhao G.S., Yu S.Z., Ren Z.Y., Variable temperature PTIR spectroscopy to study the solid-state transformation of PET/ nano CaCO3 composite materials. Spectrosc Spectr Anal, 2010, 30(02), 336-339.
8. Peng Y., Application of two-dimensional infrared correlation spectroscopy in polymer systems. PhD Thesis, Fudan University, Shanghai, 2006.
9. Wang H.F., Preparation and crystallization behavior of PET/ montmorillonite nanocomposite. Zhengzhou University, Zhengzhou, 2014
10. Deng Q.L, Liang D., Zheng Y.C., et al., Analysis of the structure and performance of nylon 56 fiber. Chem Fiber Textile Technol, 2017, 46(03), 42-46.

11. Pepin J., Gaucher V., Lefebvre J. M., Stroeks A., Biaxial stretching behavior as a probe of H-bond organization in semi-crystalline polyamides. Polymer, 2016, 101(2), 217-224.
12. Feng Z.C, Zhu B., Shi J.J., Yang X.H., Wang M.J., He P., Synthesis of four heavy H-bond chain extenders and their effects on the properties of polyurethane. Polyurethane Ind, 2011, 26(2), 5-10.
13. Litvinov V.M., Koning C.E., Tijssen J., The effect of annealing of linear and branched polyamide 46 on the phase composition, molecular mobility and water absorption as studied by DSC, 1 H and 2 H solid-state NMR. Polymer, 2015, 56(1), 406-415.
14. Li Z.H., Xin M.H., Li M.C., The advances in research on H-bonds of polymer blends. Chem Adv, 2008, 27(8), 1162-1169.
15. Wang Y.H., Cheng C., Non-isothermal crystalline kinetics and transparence of nylon 6/montmorillonite nanocomposite. Chem Res, 2011, 22(3), 51-55.
16. Li F., Preparation of polyamide 6/MMT composites from organic modification montmorillonite. Application. Appl Chem Ind, 2012, 41(4), 646-648.
17. Cui H.J., Li M. H., Li Q.Y., Carbon fiber reinforced montmorillonite modified nylon 6 composite and its manufacturing method. CN104559156A, 2015.
18. Chen Z.Y., Hay J.N., Jenkins M.J., The thermal analysis of poly (ethylene terephthalate) by FTIR spectroscopy. Thermochim Acta, 2013, 552(3), 123-130.
19. Chen Z.Y., Hay J.N., Jenkins M.J., The kinetics of crystallization of poly (ethylene terephthalate) measured by FTIR spectroscopy. Eur Polymer J, 2013, 49(6), 1722-1730.
20. Chen Z.Y., Hay J.N., Jenkins M.J., FTIR spectroscopic analysis of poly (ethylene terephthalate) on crystallization. Eur Polymer J, 2012, 48(9), 1586-1610.
21. Li D., Li D.S., Mechanical properties of nylon 6/montmorilloid nanocomposites. China Engineering Plastics Composite Technology Symposium, 2012, 1(1), 126-127.
22. Li H.J., Preparation and properties of nylon 6/nano-montmorillonite composites. China Synthetic Fiber Ind, 2013, 36(2), 34-37.
23. Zong Y., Zhang Q.H., Gu L.Q., et al., Preparation of mixed metal oxides/PA6 composite its properties. Synthetic Fiber in China, 2013, 90(3), 259-262.